Chemical Engineering Journal

Co-N-C Axially Coordination Regulated H 2 O 2 Selectivity via water medicated recombination of solute OH•: a new route
--Manuscript Draft--

Manuscript Number:	
Article Type:	Research Paper
Section/Category:	Catalysis
Keywords:	single atom catalyst; surface modification; production selectivity; reaction mechanism; dynamic simulation
Corresponding Author:	Jing Wang Yanshan University Qinhuangdao, Hebei CHINA
First Author:	Jing Wang
Order of Authors:	Jing Wang
	Junpeng Chen
	Shuang Li
	Yuan Zhao
	Jiachao Zhao
	Xinyu Liang
	Meirong Xia
	Jun Yang
	Xue Yong
	John S Tse
Abstract:	The cobalt, earth abundant transition metal, embedded in nitrogen doped carbon material as single atom site (Co-N-C) has been manifested as promising electrochemical oxygen reduction reaction (ORR) catalyst, however the unsatisfying production selectivity has hampered its widespread applications. Herein, the H2O2 selectivity of Co-N-C catalyst has been tailored with Co axial functional groups.. Thermodynamically, the selectivity is regulated due to the fine-tunning of the adsorption of the key reaction intermediates (ΔG*OOH), and five functional groups, including -O, -OH, -CN, CH3 and -SO3, endow the Co-N-C catalyst with superior H2O2 selectivity. Importantly, we unravel a new water medicated recombination of solute OH• reaction pathway for H2O2 production, which was the result of dissociation of *HOOH in explicit water environment That is two ·OH species reaction in the liquid environment which originated from the creaking of *OOH intermediates due to the weakened O-O bond by the interaction with surrounding water. This study provides foundational understanding for the ORR catalytic mechanism at the electrochemical interface and open up new avenues for rational design of targeted high efficiency electrocatalysts.

Co-N-C Axially Coordination Regulated H$_2$O$_2$ Selectivity via water medicated recombination of solute OH•: a new route

Jing Wang[a],*, Junpeng Chen[a], Shuang Li[a], Yuan Zhao[a], Jiachao Zhao[a], Xinyu Liang[a], Meirong Xia[a], Jun Yang[b],*, Xue Yong[c],*, John S Tse[d]

[a]*Hebei Key Laboratory of Heavy Metal Deep-Remediation in Water and Resource Reuse, School of Environmental and Chemistry Engineering; State Key Laboratory of Metastable Materials Science and Technology, Yanshan University, Qinhuangdao, 066004, China*

[b]*State Key Laboratory of Multiphase Complex Systems, Institute of Process Engineering Chinese Academy of Sciences, Beijing 100190, China*

[c]*Department of Electrical Engineering and Electronics,University of Liverpool*

[d]*Department of Physics, University of Saskatchewan, Saskatoon, SK, S7N 5B2, Canada*

Email: jwang6027@ysu.edu.cn(JW);   jyang@ipe.ac.cn(JY);
        Xue.yong@liverpool.ac.uk(XY)

Abstract：The cobalt, earth abundant transition metal, embedded in nitrogen doped carbon material as single atom site (Co-N-C) has been manifested as promising electrochemical oxygen reduction reaction (ORR) catalyst, however the unsatisfying production selectivity has hampered its widespread applications. Herein, the H$_2$O$_2$ selectivity of Co-N-C catalyst has been tailored with Co axial functional groups.. Thermodynamically, the selectivity is regulated due to the fine-tunning of the adsorption of the key reaction intermediates (ΔG_{*OOH}), and five functional groups, including -O, -OH, -CN, CH$_3$ and -SO$_3$, endow the Co-N-C catalyst with superior H$_2$O$_2$ selectivity. Importantly, we unravel a new water medicated recombination of solute OH• reaction pathway for H$_2$O$_2$ production, which was the result of dissociation of *HOOH in explicit water environment *That is* two ·OH species reaction in the liquid environment which originated from the creaking of *OOH intermediates due to the weakened O-O bond by the interaction with surrounding water. This study provides foundational understanding for the ORR catalytic mechanism at the electrochemical interface and open up new avenues for rational

design of targeted high efficiency electrocatalysts.

1. Introduction

The oxygen reduction reaction (ORR) involves multiple electron and and proton transferring, which proceeds either by two electrons (2e) to H_2O_2 or by four electrons (4e) to H_2O[1]. The 4e process is a key half-cell reaction in many renewable energy conversion and utilization techniques, such as polymer electrolyte membrane fuel cells and metal-air battery [2-5], while the 2e ORR has recently emerged as an alternative sustainable and environmental friendliness scheme to commercial H_2O_2 production. H_2O_2 is a versatile oxidant and is widely applied in a large range of chemical processes including paper manufacturing, wastewater treatment and medical industry, the demanding of which has ever been growing globally[6-8]. The electrochemical 2e ORR for H_2O_2 production operates in ambient condition, is safe and avoids complex procedures, huge energy consuming.[9-11]. Nevertheless, high overpotential and sluggish kinetics of the ORR have severely hampered the energy efficiency of the electrosynthesis of H_2O_2[12-18], Moreover, the competing 4e and 2e reaction pathway, intrinsically requires the development of active and selective catalyst[19] toward H_2O_2. Currently, noble-metals and their alloys manifest satisfactory performance, yet their high toxicity and reservation scarcity impedes large-scale commercial applications[20-22].

Dedicated efforts have been devoted to designing noble-metal-free electrocatalysts, among which isolated metal site embedded in nitrogen doped carbon materials (M-N-C) represent one of the most promising ORR electrocatalysts[23-30]. Benefiting from the merit of carbon materials such as high electronic conductivity, mechanical stability and structure versatility, the catalytic performance of M-N-C, (M=XXX) catalysts outperform most counterparts. Most importantly, the simple and tunable metal reaction center, which is well-accepted as MN_4 moiety, provides a representative platform to study the cooperative of metal site and its surrounding coordination atoms[31-37]. Various approaches have been established to achieve excellent catalytic performance, including heteroatom doping[31], dual/triple metal

sites[32], strain engineering[33], defect/edge modulation[34], surface modification[35-37] *etc*. For instance, the Co-N-C material has attracted wide attention because it has been proven to be promising in many scenarios and it is elusive from Fenton reaction. To further improve its ORR catalyst performance, various functional groups have been introduced at the metal site to optimize the free energy change of the *OOH reaction intermediates (ΔG_{*OOH})[6]. It is found that electron-rich groups, *i.e.*, *O and *OH, increase the value of ΔG_{*OOH}, populating it to the optimal 4.22 eV. By contrast, with electron-poor species, such as *H, the ΔG_{*OOH} is decreased and moves away from the optimal value. As far as the realistic condition is concerned, the underlying elementary steps occur at the solid-liquid interface whereby the reactants and intermediates not only interact with the catalyst substrate but also dynamically communicate with the solvent molecules[38-41]. Myriads of literature have demonstrated the significant influence of solvent environment. For instance, the rate determining step (PDS) of 2e ORR on Fe-N-C catalyst was reported to be the replacement of the preadsorbed H_2O molecule by the O_2 molecule on the Fe atom under an explicit water environment through a new reaction pathway, rather than the thermodynamically limiting step of $*O_2$ hydrogenation or *OH desorption within a vacuum model [42]. Therefore, a systematic studies on how solution environment affect the reaction product and pathways are highly required to uncover the full reaction pathways for the electrochemical synthesis H_2O_2.

Hereafter, the water effect on the selectivity for 2e reaction pathways toward H_2O_2 on Co-N-C catalyst with different axial functional groups on the Co atom was explored using DFT and *Ab initio* molecular dynamics (AIMD) simulations. (Fig. 1). 5 functional groups among the 22 candidates, including -OH, -O, -SO$_3$, -CN and -CH$_3$, is robust to regulate the reaction pathways and optimize the ΔG_{*OOH} approaching the optimal point for the formation of H_2O_2. Explicit water molecules were added to the catalysts in AIMD simulations to exploit the reaction within the interface of the catalyst surface and the liquid environment. Importantly, we observed that the *OOH intermediate is not stable under water environment (*OOH $\rightarrow$ *O + ·OH). it is thus proposed that the H_2O_2 can be formed via two ·OH reacting in the solvent, a novel

reaction pathways that has never been reported in literature. This study provides fundamental insights into the 2e reaction pathway for ORR at atomic level, which leads to new research direction for rational design of high performance catalyst.
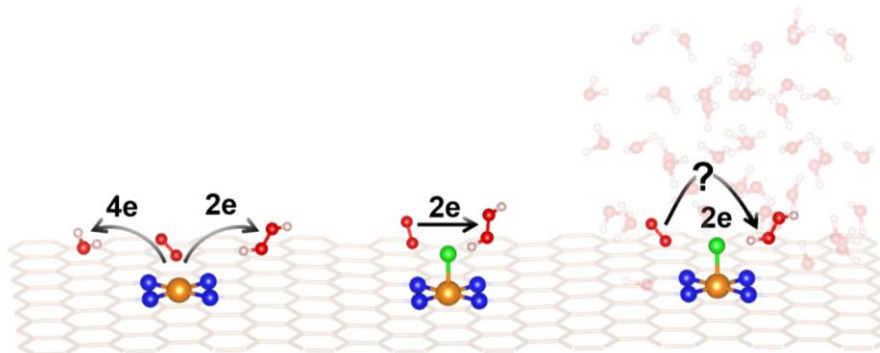

Fig. 1. Schematic of the axial functional group modification strategy to improve the production selectivity for Co-N-C catalyst with/without water environment.

2. Computation methods

The density functional theory (DFT) calculations were conducted using the Vienna Ab initio Simulation Package (VASP) software[43]. A 6 × 6 monolayer graphene supercell is utilized as the supported layer with a vacuum of 20 Å applied above the slab to avoid interlayer interactions. The effect of implicit solvation is considered via a self-consistent polarizable continuum model as implemented in VASPsol[44,45]. VASPKIT is applied for post computational data processing [46]. The equilibrium potential (U^0) of the 2e pathway is 0.70 V [Ref]. The thermodynamic overpotential $\eta^{H_2O_2}$ = |4.22 - ΔG_{*OOH}| V for a given electrocatalyst and the limiting potential $U^L = U^0 - \eta^{H_2O_2}$. Other calculation details can be found from our previous work[47].

The AIMD simulations were performed using the CP2K package. PBE functional and a hybrid Gaussian/Plane-Wave (GPW) scheme were adopted[48,49]. The cutoff energy for the plane waves expanded is 400 Rydberg. Dispersion correction was applied with the DFT-D3 method[50-52]. The canonical (NVT) ensemble AIMD are performed at 300K by employing Nose-Hoover thermostats. A time step of 1.0 fs is used [53,54] and the simulation lasts for more than 20 ps. The GTH pseudopotentials[55,56] were chosen for describing the core electrons.

3. Results and discussion

The ORR activity of Co-N-C catalyst is revisited in our study to validate our methods[37, 40]. The structures of these Co-N_C catalyst with key interaction mediates are provided in Fig. S1 and the free energy changes are displayed in Fig. S2. The free energy diagram (Fig. S2) reveals that the 4e ORR is limited by the formation of the second H_2O molecular, which is the step of *OH desorption. As shown in (Fig. 2a) and (Fig. S1), compared with the ideal value, the dark blue of ΔG_{*OH} (<. 1.0 eV) for Co-N-C suggests stronger binding energy which gives rise to an overpotential (η^{H_2O}) of 0.54 V to produce H_2O. By contrast, the 2e pathway is restricted by the formation/dissociation of *OOH intermediate, $i.e.$, the step of ΔG_{*OOH} is 3.90 eV and the deviation from the ideal value generates the overpotential ($\eta^{H_2O_2}$) of 0.30 eV. The small 0.24 eV difference in the overpotential of 4e and 2e pathways demonstrates inferior selectivity between H_2O and H_2O_2 production for Co-N-C catalyst, consistent with previous studies[40].
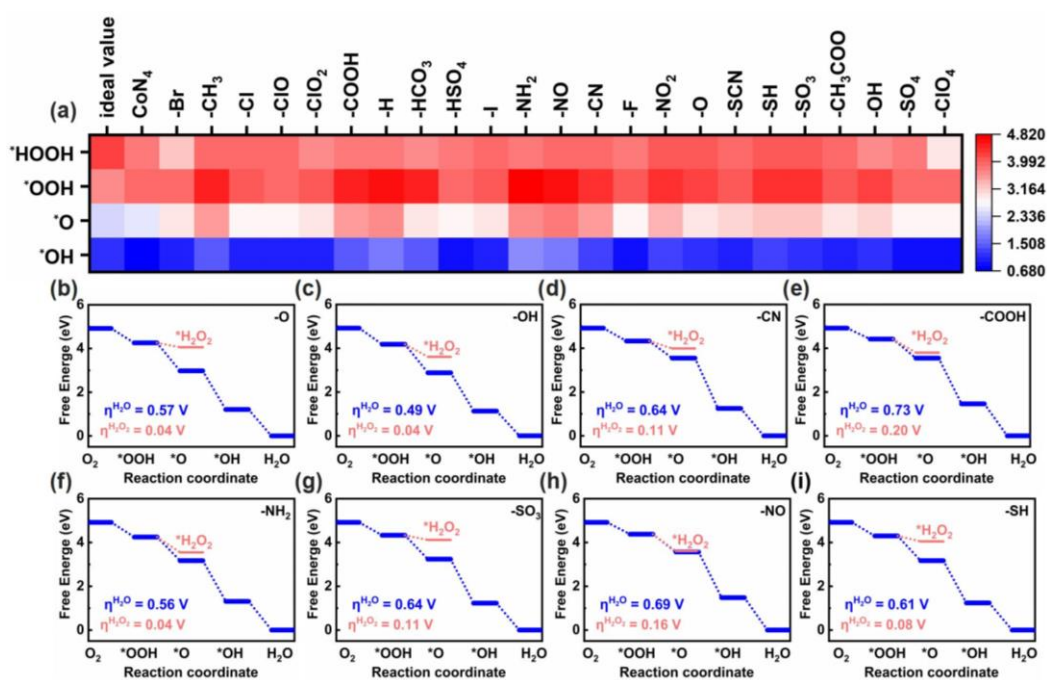

Fig. 2. (a) Free energy hotmap for key reaction intermediates with/without different axial functional group modification for Co-N-C, Free energy diagram for (b) -O (c) -OH (d) -CN (e) -COOH (f) $-NH_2$ (g) $-SO_3$ (h) -NO (i) -SH modified Co-N-C.

22 functional groups, including -Br, -CH$_3$, -CI, -ClO, -ClO$_2$, -COOH, -H, -HCO$_3$, -HSO$_4$, -I, -NH$_2$, -NO, -CN, -F, -NO$_2$, -O, -SCN, -SH, -SO$_3$, -CH$_3$COO, -OH, -SO$_4$, -ClO$_4$ were introduced axially at the Co site to tune the activity and selectivity Co-N-C catalysts. The heatmap of the free energy changes for the key reaction intermediates, *i.e.*, *OOH, *O, *OH and *HOOH for all the modified catalysts are depicted in (Fig. 2a, Fig. S1 & S2). Compared with that for Co-N-C catalyst with no axial functional groups, the color of ΔG_{*O} tends to be white or pink for the functionlized counterparts, indicating weakened interaction between the *O and the catalyst surface. A close inspection to the other two key intermediates (*OOH and *OH) for the 4e reaction pathway found similar trend. Benefiting from the alleviated interaction of *OH, the 4e activity of -Br and -HSO$_4$ is improved, that is, the ΔG_{*OH} for the -Br modification is 0.97 eV, corresponding to a smaller overpotential of 0.26 V, and the ΔG_{*OH} of 0.92 eV for the -HSO$_4$ functionlization gives rise to an overpotential of 0.31 eV (Fig. S2). For other functionalized catalysts, the potential determining steps are all changed to the first protonation step, *i.e.*, *O$_2$ → *OOH, due to the weak binding strength of XX (Fig. S2). Since activity of 2e is also dependent on the strength of ΔG_{*OOH}, the *OOH intermediate is thus the key factor for the production selectivity. The introduction of different axial functional groups resulted in the change of charge states of Co as indicated from the Bader charge analysis results. (Fig. 3a), Consequently, these Co site modified catalysts show a various range of adsorbing strength toward the *OOH intermediates with different 2e over potentials. The reaction activity of the 2e and 4e pathways of the Co site modified catalysts are summarized in (Fig. 3b-c). It is found that, with the adding of -Br, -Cl, -I, -F, -ClO, -ClO$_2$, -HSO$_4$, -SCN, -CH$_3$COO, and -OH groups, the ΔG_{*OOH} fails in 3.91 ~ 4.14 eV which boost the 4e reaction pathway. In contrast, with the -CH$_3$, -COOH, -HCO$_3$, -CN, -NO$_2$, -O, -SH, and -SO$_3$ groups, ΔG_{*OOH} further increase to 4.05 ~ 4.42 eV, the 2e pathway become favorite reaction pathways. It is noticed that in the region with ΔG_{*OOH} 4.05 ~ 4.14 eV, both 2e and 4e reaction pathways are active but lacking selectivity. By contract, the 4e selectivity is dominate when ΔG_{*OOH} is in the range of 3.91 ~ 4.05 eV, yet the 2e overwhelms with ΔG_{*OOH} 4.14 ~ 4.42 eV. Specifically, eight

functionalized catalysts are found with promising 2e selectivity (Fig. 2b-i).

To provide a general trend of the regulations, the limiting potential (U^L) of the 2e and 4e reactions has been depicted in (Fig. 4a). The pink line demonstrates the same U^L for 2e and 4e pathways, and thus the left upper triangle suggests better 2e activity while the other one on the right bottom manifests 4e pathways. Further, taking the U^L (0.78 V) of commercial Pt/C for 4e pathway and $U^L = 0.5$ V for 2e pathways as the benchmark, the purple rectangle circled on the left upper shows superior 2e selectivity and activity, which exhibits small 2e overpotential but large 4e overpotential. The eight candidates found in these region are those mentioned above that with improved 2e activity but depressed 4e efficiency. On the contrary, the pink trapezoid on the right bottom reveals 4e selectivity and activity; however, unfortunately, no point is witnessed there. In the light blue and dark blue regions, although the catalysts show both 2e and 4e activities, the lack of selectivity hinders its real application.
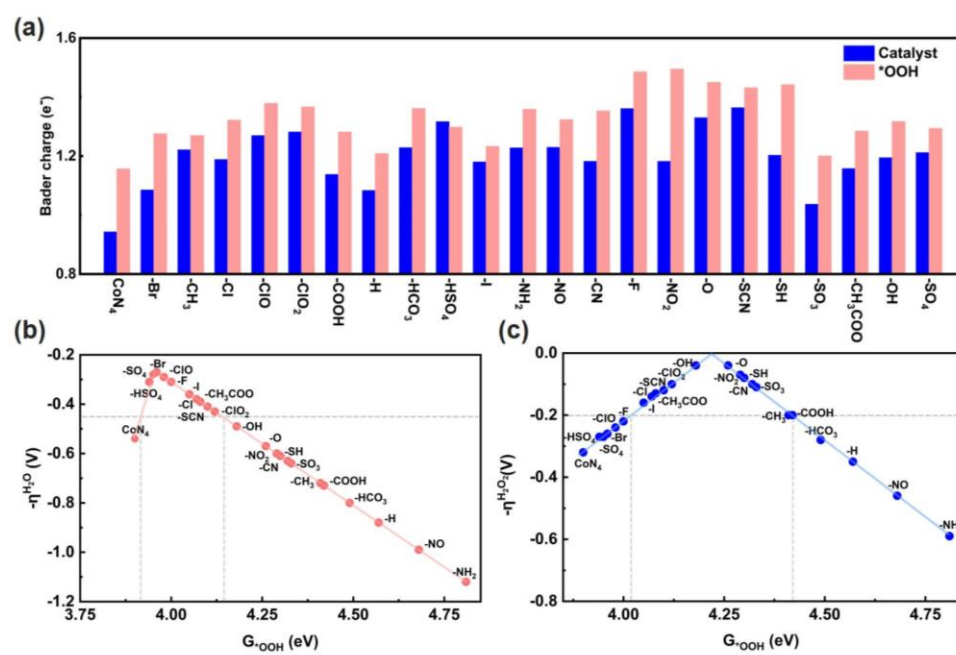
Fig. 3. (a) Bader charge for the metal in the catalyst and the *OOH intermediate. Volcano plot for (b) 4e activity and (c) 2e activity related to ΔG_{*OOH}.

The above calculations had been done in vacuum model, which doesn't include water environment effect. The solvent effect was thus implicitly considered for both accurate and efficient concerns. As depicted in (Fig. 4b), clear discrepancies can be

found between the vacuum model to the implicit solvation model. For example, -NO and -NH$_2$ groups functionalized catalysts are found in the left upper purple region in the solvation model, which are located in the left corner in the vacuum model, yet the -COOH, -HCO$_3$, -NO$_2$ and -SH containing cases are moved out from the purple region. That is, six functional groups are beneficial for Co-N-C to show desirable 2e selectivity in solvation model, and among them the promising of -OH, -O, -SO$_3$, -CN and -CH$_3$ modified cases are robust in both models. Moreover, one point can be found in the pink region, which is the -SCN functionalized catalyst, demonstrating excellent 4e activity and selectivity.
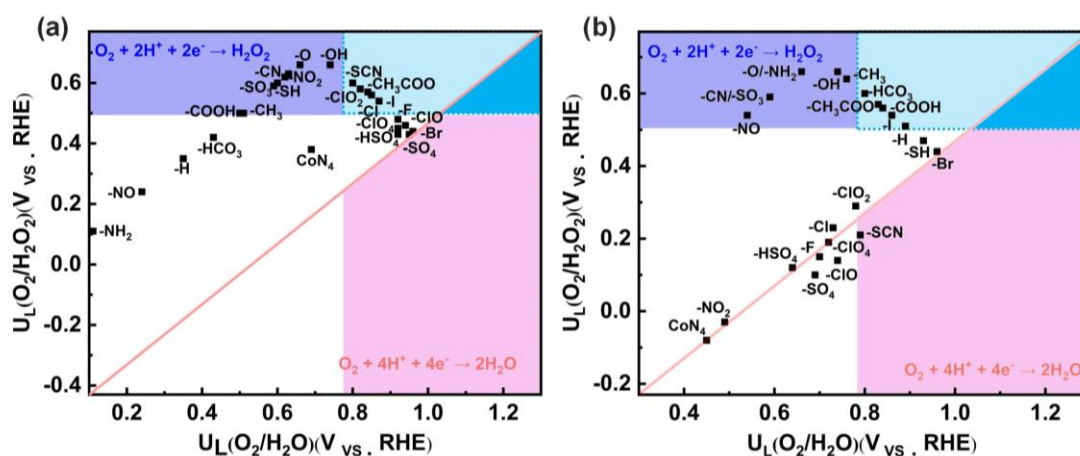
Fig. 4. Two-dimensional map for the 2e and 4e selectivity for axial functional groups modified Co-N-C catalyst. (a) vacuum model, (b) implicit solvation model.

The large discrepancy of the vacuum and implicit solvation models demonstrate that the impact of the solvation on the selectivity is significant. Moreover, the ORR activity of Co-N-C is inferior in the solvation model, which sites at the left bottom of (Fig. 3b), inconsistent with the previous experimental studies[1]. These facts underline the complex behaviour in the vicinity of the solid/liquid interface and stimulate us to perform AIMD simulations with explicit solvation via exposing the catalyst to finite water molecules, with/without axial functional groups. The representative snapshots from AIMD simulation for each key intermediate are shown in (Fig. 5) (corresponding movies can be found in Movie I file). For the bare Co-N-C, the *OOH and *OH intermediates stay stable during the 10 ps simulation without any

desorption, suggesting strong chemisorption for the binding. The *O intermediate is prone to capture a proton from the water molecule nearby, and quickly transforms into an adsorbed hydroxyl and a free OH in the liquid water. This is consistent with previous reported results[39]. Importantly, the *HOOH intermediate is found to be unstable in the explicit water environment, whereby the O-O bond is weakened by the surrounded water molecules through hydrogen bonds, and quickly dissociates into *OH species and a OH• species. This is contradicted to the formation of H_2O_2, while H_2O_2 was observed the product in experiments. This controversy inspires us to explore the mechanism for the formation of H_2O_2 under aqueous medium.

An in-depth check of the chemical status for the generated OH species suggest that the OH species is extremely active which can uptake a proton from the neighboring water molecular, and then the newly formed OH tends to trap another proton from water molecular, triggering a chain reaction and forming a long-distance interaction (Movie II file). It is thus speculated that the OH species is a radical. Consequently, the H_2O_2 can be formed when the two OH radicals encounter each other in the aqueous medium. That is, a new electrocatalytic mechanism is proposed as follows, (i) $* + O_2 \rightarrow *O_2$, (ii) $*O_2 + H^+ + e \rightarrow *OOH$, (iii) $*OOH + H^+ + e \rightarrow *O +H_2O$, (iv) $*O + H_2O \rightarrow *OH + \cdot OH$, (v) $2 \cdot OH \rightarrow H_2O_2$. To give more evidence for the supposed mechanism, we further conduct the AIMD simulation for the -OH functionalized Co-N-C (Fig. 5b & Movie II file), and it is found that the *HOOH intermediate also decompose into *OH and OH species, similar to the bare counterpart. This further demonstrates that the H_2O_2 can be generated from the solvent via two ·OH reaction.

Encouraged by the proposed reaction pathways, the AIMD simulations are extended to Co-N-C catalyst with -O, -CN, -SO₃, -NO, -CH₃ and -NH₂ groups, which show excellent 2e activity and selectivity in implicit solvation model. It is found that the *HOOH intermediate is not stable for the catalyst with -O, -CN, -SO₃ and -NO groups (Fig. 5c & Movie III file), which desorbs from the metal site and form free H_2O_2 as in most reported catalysts[36]. By contrary, the *HOOH dissociates into *OH and OH species for Co-N-C with -NH₂, another case that the H_2O_2 is formed from

the ·OH radicals in the water, alike the bare and -OH modified catalysts.

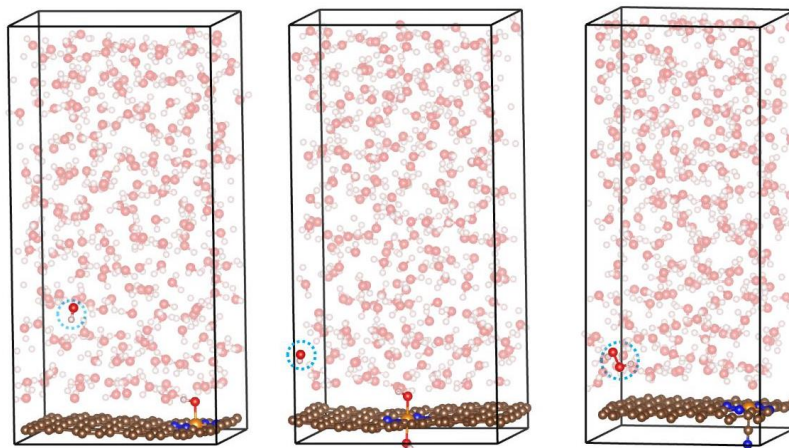**Fig. 5.** MD Snapshots of the creaking/desorption of the *HOOH reaction intermediates for (a) bare (b) -OH modified (c) -CN modified Co-N-C catalyst.

4. Conclusion

In conclusion, the activity and selectivity of the model catalyst Co-N-C have been regulated systematically via axial coordinators binding at the Co site, through the combination of density functional theory and *ab initio* molecular dynamic simulations. It is found that all the utilized functional groups tend to alleviate the binding of the key reaction intermediates, and with elaborate selection of suitable candidates, the free energy of the key reaction intermediate, say ΔG_{*OOH}, can be tailored to promote the 2e selectivity, which suppresses the 4e reaction pathway with small 2e overpotential. Dynamic simulations reveal that the *OOH is unstable for Co-N-C catalyst under the interaction of neighboring water molecular, and the H_2O_2 can be generated through the ·OH species in the aqueous media. This study displays fundamental importance of solid-liquid interfacial microenvironment in governing the electrocatalytic reaction mechanism, opening up unique avenues for rational design of high performance catalysts from the full concern of the reaction environment.

Reference

[1] S. Chen, T. Luo, X. Li, K. Chen, J. Fu, K. Liu, C. Cai, Q. Wang, H. Li, Y. Chen, C. Ma, L. Zhu, Y.-R. Lu, T.-S. Chan, M. Zhu, E. Cortés, M. Liu, Identification of the Highly Active Co–N$_4$ Coordination Motif for Selective Oxygen Reduction to Hydrogen Peroxide, J. Am. Chem. Soc. 144(32) (2022) 14505-14516. https://doi.org/10.1021/jacs.2c01194.

[2] W. Xiang, N. Yang, X. Li, J. Linnemann, U. Hagemann, O. Ruediger, M. Heidelmann, T. Falk, M. Aramini, S. DeBeer, M. Muhler, K. Tschulik, T. Li, 3D atomic-scale imaging of mixed Co-Fe spinel oxide nanoparticles during oxygen evolution reaction, Nat. Commun. 13(1) (2022) 179. https://doi.org/10.1038/s41467-021-27788-2.

[3] Z.Z. Liang, H.Y. Wang, H.Q. Zheng, W. Zhang, R. Cao, Porphyrin-based frameworks for oxygen electrocatalysis and catalytic reduction of carbon dioxide, Chem. Soc. Rev. 50(4) (2021) 2540-2581. https://doi.org/10.1039/d0cs01482f.

[4] N. Karmodak, J.K. Nørskov, Activity And Stability of Single- And Di- Atom Catalysts for the O$_2$ Reduction Reaction, Angew. Chem. Int. Ed. 62(47) (2023) e202311113. https://doi.org/10.1002/anie.202311113.

[5] J. Meng, Y. Song, Z. Qin, Z. Wang, X. Mu, J. Wang, X.X. Liu, Cobalt–Nickel Double Hydroxide toward Mild Aqueous Zinc- Ion Batteries, Adv. Funct. Mater. 32(33) (2022) 2204026. https://doi.org/10.1002/adfm.202204026.

[6] E. Jung, H. Shin, B.-H. Lee, V. Efremov, S. Lee, H.S. Lee, J. Kim, W. Hooch Antink, S. Park, K.-S. Lee, S.-P. Cho, J.S. Yoo, Y.-E. Sung, T. Hyeon, Atomic-level tuning of Co–N–C catalyst for high-performance electrochemical H$_2$O$_2$ production, Nat. Mater 19(4) (2020) 436-442. https://doi.org/10.1038/s41563-019-0571-5.

[7] J. Du, G. Han, W. Zhang, L. Li, Y. Yan, Y. Shi, X. Zhang, L. Geng, Z. Wang, Y. Xiong, G. Yin, C. Du, CoIn dual-atom catalyst for hydrogen peroxide production via oxygen reduction reaction in acid, Nat. Commun. 14(1) (2023) 4766. https://doi.org/10.1038/s41467-023-40467-8.

[8] Y. Tian, M. Li, Z. Wu, Q. Sun, D. Yuan, B. Johannessen, L. Xu, Y. Wang, Y. Dou,

H. Zhao, S. Zhang, Edge- hosted Atomic Co−N$_4$ Sites on Hierarchical Porous Carbon for Highly Selective Two- electron Oxygen Reduction Reaction, Angew. Chem. Int. Ed. 61(51) (2022) e202213296. https://doi.org/10.1002/anie.202213296.

[9] M. Karimi, R. Borthakur, C.L. Dorsey, C.-H. Chen, S. Lajeune, F.P. Gabbaï, Bifunctional Carbenium Dications as Metal-Free Catalysts for the Reduction of Oxygen, J. Am. Chem. Soc. 142(32) (2020) 13651-13656. https://doi.org/10.1021/jacs.0c04841.

[10] C.W. Machan, Advances in the Molecular Catalysis of Dioxygen Reduction, ACS Catalysis 10(4) (2020) 2640-2655. https://doi.org/10.1021/acscatal.9b04477.

[11] E. Jung, H. Shin, W. Hooch Antink, Y.-E. Sung, T. Hyeon, Recent Advances in Electrochemical Oxygen Reduction to H$_2$O$_2$: Catalyst and Cell Design, ACS Energy Letters 5(6) (2020) 1881-1892. https://doi.org/10.1021/acsenergylett.0c00812.

[12] K. Jiang, J. Zhao, H. Wang, Catalyst design for electrochemical oxygen reduction toward hydrogen peroxide, Adv. Funct. Mater. 30(35) (2020) 2003321. https://doi.org/10.1002/adfm.202003321.

[13] Y. Wang, G.I. Waterhouse, L. Shang, T. Zhang, Electrocatalytic oxygen reduction to hydrogen peroxide: From homogeneous to heterogeneous electrocatalysis, Adv. Energy Mater. 11(15) (2021) 2003323. https://doi.org/10.1002/aenm.202003323.

[14] C. Zhang, L. Yuan, C. Liu, Z. Li, Y. Zou, X. Zhang, Y. Zhang, Z. Zhang, G. Wei, C. Yu, Crystal Engineering Enables Cobalt-Based Metal–Organic Frameworks as High-Performance Electrocatalysts for H$_2$O$_2$ Production, J. Am. Chem. Soc. 145(14) (2023) 7791-7799. https://doi.org/10.1021/jacs.2c11446.

[15] B. Lv, X. Li, K. Guo, J. Ma, Y. Wang, H. Lei, F. Wang, X. Jin, Q. Zhang, W. Zhang, R. Long, Y. Xiong, U.P. Apfel, R. Cao, Controlling Oxygen Reduction Selectivity through Steric Effects: Electrocatalytic Two- Electron and Four- Electron Oxygen Reduction with Cobalt Porphyrin Atropisomers, Angew. Chem. Int. Ed. 60(23) (2021) 12742-12746. https://doi.org/10.1002/anie.202102523.

[16] J. Zhang, J. Yang, Y. Wang, H. Lu, M. Zhang, Catalytic mechanism of oxygen reduction on two types of CoN$_4$-graphene: A density functional study, Int.J. Energ. Res 45(7) (2021) 10858-10868. https://doi.org/10.1002/er.6570.

[17] F. Ai, J. Wang, Insights into the Electrochemical Production of Hydrogen Peroxide over Single-Atom Co–N–C Catalysts with the Introduction of Carbon Vacancy Defect near the Co–N$_4$ Site, The Journal of Physical Chemistry Letters 14(15) (2023) 3658-3668. https://doi.org/10.1021/acs.jpclett.3c00044.

[18] W. Liu, C. Zhang, J. Zhang, X. Huang, M. Song, J. Li, F. He, H. Yang, J. Zhang, D. Wang, Tuning the atomic configuration of Co-N-C electrocatalyst enables highly-selective H$_2$O$_2$ production in acidic media, Appl. Catal., B 310 (2022) 121312. https://doi.org/10.1016/j.apcatb.2022.121312.

[19] J. Liu, Z. Wei, Z. Gong, M. Yan, Y. Hu, S. Zhao, G. Ye, H. Fei, Single-atom CoN$_4$

sites with elongated bonding induced by phosphorus doping for efficient H_2O_2 electrosynthesis, Appl. Catal., B 324 (2023). https://doi.org/10.1016/j.apcatb.2022.122267.

[20] Y. Xue, Y. Wang, Z. Pan, K. Sayama, Electrochemical and photoelectrochemical water oxidation for hydrogen peroxide production, Angew. Chem. Int. Ed. 60(19) (2021) 10469-10480. https://doi.org/10.1002/anie.202011215.

[21] H.W. Kim, M.B. Ross, N. Kornienko, L. Zhang, J. Guo, P. Yang, B.D. McCloskey, Efficient hydrogen peroxide generation using reduced graphene oxide-based oxygen reduction electrocatalysts, Nat. Catal. 1(4) (2018) 282-290. https://doi.org/10.1038/s41929-018-0044-2.

[22] S. Siahrostami, A. Verdaguer-Casadevall, M. Karamad, D. Deiana, P. Malacrida, B. Wickman, M. Escudero-Escribano, E.A. Paoli, R. Frydendal, T.W. Hansen, Enabling direct H_2O_2 production through rational electrocatalyst design, Nat. Mater 12(12) (2013) 1137-1143. https://doi.org/10.1038/NMAT3795.

[23] A. Verdaguer-Casadevall, D. Deiana, M. Karamad, S. Siahrostami, P. Malacrida, T.W. Hansen, J. Rossmeisl, I. Chorkendorff, I.E. Stephens, Trends in the electrochemical synthesis of H_2O_2: enhancing activity and selectivity by electrocatalytic site engineering, Nano Lett. 14(3) (2014) 1603-1608. https://doi.org/10.1021/nl500037x.

[24] F. Zheng, Y. Ji, H. Dong, C. Liu, S. Chen, Y. Li, Edge effect promotes graphene-confining single-atom $Co–N_4$ and $Rh–N_4$ for bifunctional oxygen electrocatalysis, J. Phys. Chem. C 126(1) (2021) 30-39. https://doi.org/10.1021/acs.jpcc.1c07691.

[25] W. Zhang, Y. Chao, W. Zhang, J. Zhou, F. Lv, K. Wang, F. Lin, H. Luo, J. Li, M. Tong, Emerging dual- atomic- site catalysts for efficient energy catalysis, Adv. Mater. 33(36) (2021) 2102576. https://doi.org/10.1002/adma.202102576.

[26] J. Yan, F. Ye, Q. Dai, X. Ma, Z. Fang, L. Dai, C. Hu, Recent progress in carbon-based electrochemical catalysts: From structure design to potential applications, Nano Res. Energy 2(2) (2023) e9120047. https://doi.org/10.26599/nre.2023.9120047.

[27] Y. Sun, J. Wang, Q. Liu, M. Xia, Y. Tang, F. Gao, Y. Hou, J. Tse, Y. Zhao, Itinerant ferromagnetic half metallic cobalt–iron couples: promising bifunctional electrocatalysts for ORR and OER, J. Mater. Chem. A 7(47) (2019) 27175-27185. https://doi.org/10.1039/C9TA08616A.

[28] P. Li, Y. Jiao, Y. Ruan, H. Fei, Y. Men, C. Guo, Y. Wu, S. Chen, Revealing the role of double-layer microenvironments in pH-dependent oxygen reduction activity over metal-nitrogen-carbon catalysts, Nat. Commun. 14(1) (2023). https://doi.org/10.1038/s41467-023-42749-7.

[29] X. Zhao, R. Zhao, Q. Liu, H. Chen, J. Wang, Y. Hu, Y. Li, Q. Peng, J.S. Tse, A p-d block synergistic effect enables robust electrocatalytic oxygen evolution, Chin. Chem. Lett. (2024) 109496. https://doi.org/10.1016/j.cclet.2024.109496.

[30] J. Wang, H.G. Li, S.H. Liu, Y.F. Hu, J. Zhang, M.R. Xia, Y.L. Hou, O. Tse, J.J. Zhang, Y.F. Zhao, Turning on Zn 4s Electrons in a N_2-Zn-B_2 Configuration to Stimulate Remarkable ORR Performance, Angew. Chem. Int. Ed. 60(1) (2021)

181-185. https://doi.org/10.1002/anie.202009991.

[31] J. Wang, C. Liu, S. Li, Y. Li, Q. Zhang, Q. Peng, S.T. John, Z. Wu, Advanced electrocatalysts with Dual-metal doped carbon Materials: Achievements and challenges, Chem. Eng. J. 428 (2022) 132558. https://doi.org/10.1016/j.cej.2021.132558.

[32] R. Li, D. Wang, Superiority of dual- atom catalysts in electrocatalysis: one step further than single- atom catalysts, Adv. Energy Mater. 12(9) (2022) 2103564. https://doi.org/10.1002/aenm.202103564.

[33] Y. Yuan, Q. Zhang, L. Yang, L.G. Wang, W.B. Shi, P.F. Liu, R. Gao, L.R. Zheng, Z.W. Chen, Z.Y. Bai, Facet Strain Strategy of Atomically Dispersed Fe-N-C Catalyst for Efficient Oxygen Electrocatalysis, Adv. Funct. Mater. 32(36) (2022) 2206081. https://doi.org/10.1002/adfm.202206081.

[34] Y.S. Qiu, R. Gao, W.Y. Yang, L. Huang, Q.J. Mao, J.B. Yang, L.M. Sun, Z.B. Hu, X.F. Liu, Understanding the Enhancement Mechanism of A-Site-Deficient La_xNiO_3 as an Oxygen Redox Catalyst, Chem. Mater. 32(5) (2020) 1864-1875. https://doi.org/10.1021/acs.chemmater.9b04287.

[35] Y. Wang, S. LIu, X. Hao, S. Luan, H. You, J. Zhou, D. Song, D. Wang, H. Li, F. Gao, Surface reorganization engineering of the N-doped MoS_2 heterostructures MoO_x@N-doped MoS_2−x by in situ electrochemical oxidation activation for efficient oxygen evolution reaction, J. Mater. Chem. A 7(17) (2019) 10572-10580. https://doi.org/10.1039/C9TA01049A.

[36] Y. Chen, S. Ji, S. Zhao, W. Chen, J. Dong, W.-C. Cheong, R. Shen, X. Wen, L. Zheng, A. Rykov, Enhanced oxygen reduction with single-atomic-site iron catalysts for a zinc-air battery and hydrogen-air fuel cell, Nat. Commun. 9(1) (2018) 5422. https://doi.org/10.1038/s41467-018-07850-2.

[37] B. Li, C. Zhao, J. Liu, Q. Zhang, Electrosynthesis of Hydrogen Peroxide Synergistically Catalyzed by Atomic Co–N_x–C Sites and Oxygen Functional Groups in Noble- Metal- Free Electrocatalysts, Adv. Mater. 31(35) (2019) 1808173. https://doi.org/10.1002/adma.201808173.

[38] L. Yan, C. Wang, Y. Wang, Y. Wang, Z. Wang, L. Zheng, Y. Lu, R. Wang, G. Chen, Optimizing the binding of the *OOH intermediate via axially coordinated Co-N_5 motif for efficient electrocatalytic H_2O_2 production, Appl. Catal., B 338 (2023) 123078. https://doi.org/10.1016/j.apcatb.2023.123078.

[39] J. W. Chen, Z. S. Zhang, H. M. Yan, G. J. Xia, H. Cao, Y.G. Wang, Pseudo-adsorption and long-range redox coupling during oxygen reduction reaction on single atom electrocatalyst, Nat. Commun.13 (2022) 1734. https:// https://doi.org/10.1038/s41467-022-29357-7.

[40] E. Jung, H. Shin, B.-H. Lee, V. Efremov, S. Lee, H.S. Lee, J. Kim, W. Hooch Antink, S. Park, K.-S. Lee, Atomic-level tuning of Co–N–C catalyst for high-performance electrochemical H_2O_2 production, Nat. Mater 19(4) (2020) 436-442. https://doi.org/10.1038/s41563-019-0571-5.

[41] J. Meng, Y. Song, J. Wang, P. Hei, C. Liu, M. Li, Y. Lin, X.-X. Liu, A salt-concentrated electrolyte for aqueous ammonium-ion hybrid batteries, Chem. Sci 15 (2024) 220-229. https://doi.org/10.1039/d3sc05318k.

[42] J.-C. Liu, F. Luo, J. Li, Electrochemical Potential-Driven Shift of Frontier Orbitals in M–N–C Single-Atom Catalysts Leading to Inverted Adsorption Energies, J. Am. Chem. Soc. 145(46) (2023) 25264-25273. https://doi.org/10.1021/jacs.3c08697.

[43] J.P. Perdew, K. Burke, M. Ernzerhof, Generalized gradient approximation made simple, Phys. Rev. Lett. 77(18) (1996) 3865. https://doi.org/10.1103/PhysRevLett.77.3865.

[44] K. Mathew, V. Kolluru, S. Mula, S.N. Steinmann, R.G. Hennig, Implicit self-consistent electrolyte model in plane-wave density-functional theory, J. Chem. Phys. 151(23) (2019) 234101. https://doi.org/10.1063/1.5132354.

[45] K. Mathew, R. Sundararaman, K. Letchworth-Weaver, T. Arias, R.G. Hennig, Implicit solvation model for density-functional study of nanocrystal surfaces and reaction pathways, J. Chem. Phys. 140(8) (2014) 084106. https://doi.org/10.1063/1.4865107.

[46] V. Wang, N. Xu, J.-C. Liu, G. Tang, W.-T. Geng, VASPKIT: A user-friendly interface facilitating high-throughput computing and analysis using VASP code, Comput. Phys. Commun. 267 (2021) 108033. https://doi.org/10.17632/v3bvcypg9v.1.

[47] J. Wang, K. Li, R. Xu, S. Li, Y. Li, M.R. Xia, J.S. Tse, Z.J. Wu, Rational design of the first and second coordination spheres for copper single-atom catalyst to boost highly efficient oxygen reduction, Appl. Surf. Sci. 605 (2022) 154832. https://doi.org/10.1016/j.apsusc.2022.154832.

[48] T.D. Kühne, M. Iannuzzi, M. Del Ben, V.V. Rybkin, P. Seewald, F. Stein, T. Laino, CP2K: An electronic structure and molecular dynamics software package - Quickstep: Efficient and accurate electronic structure calculations, J. Chem. Phys. 152(19) (2020) 194103. https://doi.org/10.1063/5.0007045.

[49] P.E. Blöchl, Projector augmented-wave method, Phys. Rev. B 50(24) (1994) 17953. https://doi.org/10.1103/PhysRevB.50.17953.

[50] A. Antony, C. Hakanoglu, A. Asthagiri, J.F. Weaver, Dispersion-corrected density functional theory calculations of the molecular binding of n-alkanes on Pd(111) and PdO(101), J. Chem. Phys. 136(5) (2012) 107. https://doi.org/10.1063/1.3679167.

[51] L.M. Azofra, D.R. MacFarlane, C.H. Sun, A DFT study of planar vs. corrugated graphene-like carbon nitride (g-C_3N_4) and its role in the catalytic performance of CO_2 conversion, PCCP 18(27) (2016) 18507-18514. https://doi.org/10.1039/c6cp02453j.

[52] S. Grimme, J. Antony, S. Ehrlich, H. Krieg, A consistent and accurate ab initio parametrization of density functional dispersion correction (DFT-D) for the 94 elements H-Pu, J. Chem. Phys. 132(15) (2010) 154104. https://doi.org/10.1063/1.3382344.

[53] W.G. Hoover, Canonical dynamics: Equilibrium phase-space distributions, Phys. Rev. A 31(3) (1985) 1695. https://doi.org/10.1103/PhysRevA.31.1695.

[54] G.J. Martyna, M.L. Klein, M. Tuckerman, Nosé–Hoover chains: The canonical ensemble via continuous dynamics, J. Chem. Phys. 97(4) (1992) 2635-2643.

https://doi.org/10.1063/1.463940.

[55] S. Goedecker, M. Teter, J. Hutter, Separable dual-space Gaussian pseudopotentials, Phys. Rev. B 54(3) (1996) 1703. https://doi.org/10.1103/PhysRevB.54.1703.

[56] C. Hartwigsen, S. Gœdecker, J. Hutter, Relativistic separable dual-space Gaussian pseudopotentials from H to Rn, Phys. Rev. B 58(7) (1998) 3641. https://doi.org/10.1103/PhysRevB.58.3641.

Click here to access/download
Supplementary Material
SI_0117_mini.doc

*OOH

Click here to access/download
Video
Movie_1.mp4

*O

Click here to access/download
Video
Movie_2.mp4

*OH

Click here to access/download
Video
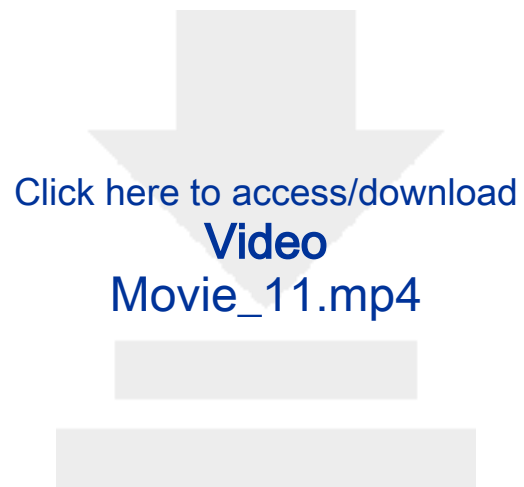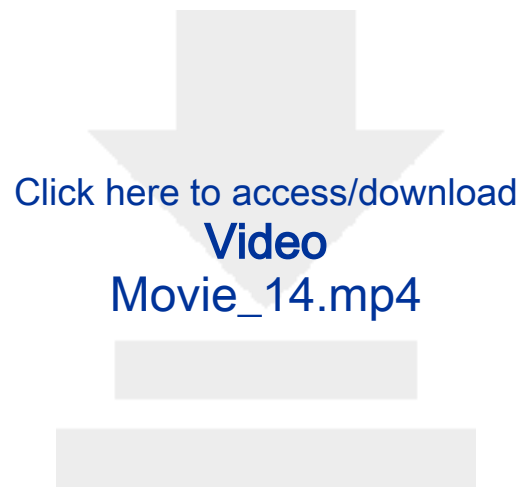Movie_3.mp4

Click here to access/download
Video
Movie_4.mp4

OH modified *OOH

Click here to access/download
Video
Movie_5.mp4

OH modified *O
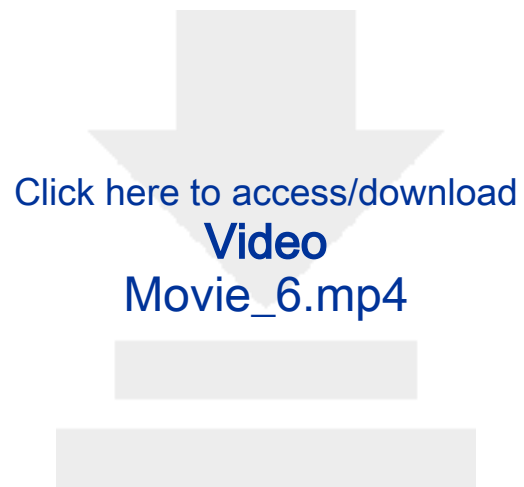
Click here to access/download
Video
Movie_6.mp4

OH modified *OH

Click here to access/download
Video
Movie_7.mp4

OH modified *HOOH
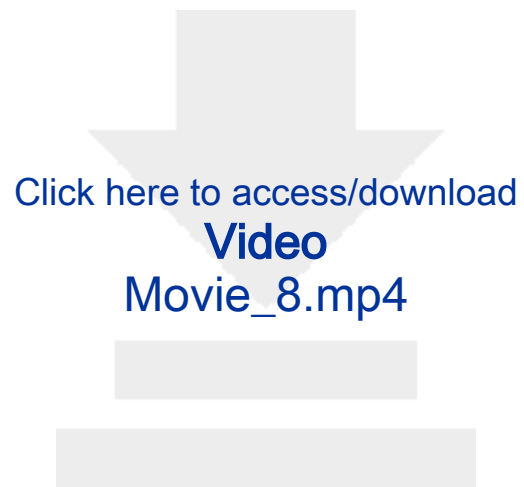
Click here to access/download
Video
Movie_8.mp4

CH3 modified *HOOH
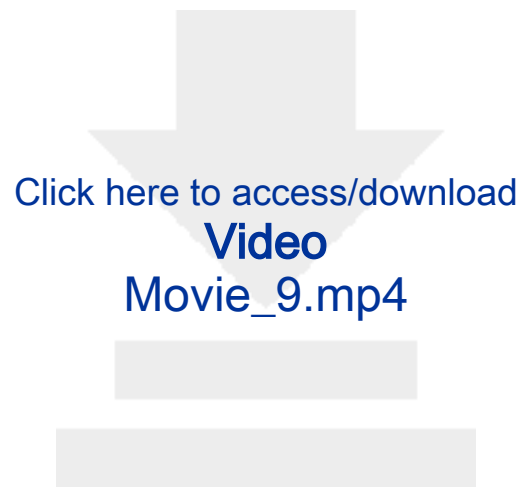
Click here to access/download
Video
Movie_9.mp4

CN modified *HOOH

Click here to access/download
Video
Movie_10.mp4

NH2 modified *HOOH

Click here to access/download
Video
Movie_11.mp4

NO modified *HOOH

Click here to access/download
Video
Movie_12.mp4

O modified *HOOH

Click here to access/download
Video
Movie_13.mp4

SO3 modified *HOOH

Click here to access/download
Video
Movie_14.mp4

Declaration of interests

☐The authors declare that they have no known competing financial interests or personal relationships that could have appeared to influence the work reported in this paper.

☒The authors declare the following financial interests/personal relationships which may be considered as potential competing interests: